HHS Public Access

Author manuscript

J Antibiot (Tokyo). Author manuscript; available in PMC 2016 December 15.

Published in final edited form as:

J Antibiot (Tokyo). 2016 July ; 69(7): 567–570. doi:10.1038/ja.2016.66.

Methyltransferases excised from *trans*-AT polyketide synthases operate on *N*-acetylcysteamine-bound substrates

D. Cole Stevens[#1], **Drew T. Wagner**[#1], **Hannah R. Manion**[1], **Bradley K. Alexander**[1], and **Adrian T. Keatinge-Clay**[1,2,*]

[1]Department of Molecular Biosciences, The University of Texas at Austin, Austin, Texas, USA

[2]Department of Chemistry, The University of Texas at Austin, Austin, Texas, USA

[#] These authors contributed equally to this work.

Keywords

methyltransferase; polyketide; trans-AT PKS; bacillaene; difficidin; mupirocin

INTRODUCTION

Trans-acyltransferase polyketide synthases (*trans*-AT PKSs) construct biologically active polyketides, such as the antibiotic mupirocin, in an assembly line process catalyzed by collections of enzymatic domains termed modules. Each module of a *trans*-AT possesses an acyl carrier protein (ACP) and ketosynthase (KS) that, along with a separately-encoded acyltransferase (AT) domain, constitute the minimal trio of domains required for the extension of a covalently-bound intermediate.[1,2] Further modifications at the α- and β-carbons of the polyketide are introduced by processing enzymes such as the methyltransferase (MT), ketoreductase (KR), dehydratase (DH), and enoylreductase (ER), depending on their inclusion within a module. This optional incorporation can be primarily credited for the vast chemical and functional diversity observed within polyketides.[1,2]

Unlike the embedded AT domains of *cis*-AT PKS pathways that deliver malonyl-CoA or methylmalonyl-CoA extender units to a single module, the discrete ATs of *trans*-AT PKSs deliver extender units to several modules. Since these ATs are primarily selective for malonyl groups, *trans*-AT PKSs employ embedded *S*-adenosyl methionine (SAM)-dependent MT domains to install methyl groups into polyketide backbones.[1-3] Although SAM-dependent MTs constitute a well-studied superfamily of enzymes and are relatively common within *trans*-AT PKSs, a dearth of information exists for *trans*-AT MTs and PKS-embedded MTs in general. Only a few studies of MTs from select *cis*-AT PKSs and fungal highly-reducing PKSs (HR-PKSs) have been reported.[4-9] Analysis of a fungal HR-PKS

[*] *Corresponding Author* adriankc@utexas.edu.

Author Contributions

All authors have given approval to the final version of the manuscript.

responsible for the production of lovastatin revealed the kinetic preference of an embedded MT towards its native acyl-*S*-*N*-acetylcysteamine (NAC) substrate analog.[1,2,9,10,11]

To explore the selectivity of *trans*-AT MTs, we examined the methylation activity of excised MT domains from three well-known *trans*-AT pathways, responsible for the production of the antimicrobial agents bacillaene, difficidin, and mupirocin (Figure 1), towards the acyl-*S*-NAC substrates 3-oxobutanoyl-*S*-NAC (**1**), 3-oxopentanoyl-*S*-NAC (**2**), and 3-oxohexanoyl-*S*-NAC (**3**).[12-14] (Figure 2a). This is the first account of the substrate specificity and activity of excised MT domains from *trans*-AT PKSs.

MATERIAL AND METHODS

S-adenosyl-methionine (Ark Pharm, Inc.) was dissolved in 300 mM sodium phosphate buffer (pH 7.8) to a final concentration of 150 mM.

The DNA encoding DifMT1, DifMT6, DifMT13, BaeMT9, BaeMT14, MupMT1, and MupMT3 was amplified from the difficidin and bacillaene gene clusters of *Bacillus amyloliquefaciens* FZB42 and the mupirocin gene cluster of *Pseudomonas fluorescens* 13525 and inserted into pGAY28b, a ligation-independent cloning vector constructed from pET28b (Table S1).[15] *E. coli* BL21(DE3) transformed with the expression plasmid was inoculated into LB media containing 50 mg/L kanamycin at 37 °C, grown to OD_{600} = 0.5, and induced with 0.5 mM IPTG. After 18 h at 15 °C, cells were collected by centrifugation and resuspended in lysis buffer (0.5 M NaCl, 10% (v/v) glycerol, 0.1 M HEPES, pH 7.5). Following sonication, cell debris was removed by centrifugation (30,000 × g, 30 min). The supernatant was poured over a column of Nickel-NTA resin (Thermoscientific), which was then washed with 40 mL lysis buffer containing 15 mM imidazole and eluted with 5 mL lysis buffer containing 150 mM imidazole. The eluted protein was concentrated to ~10 mg/mL in the equilibration buffer and stored at −80 °C until needed. The *S*-adenosyl-homocysteine (SAH) nucleosidase Pfs was amplified from *E. coli* BL21(DE3) genomic DNA and cloned and purified as above (Table S1). Reactions were supplemented with Pfs due to the potent inhibition of MTs by SAH.[5]

Compounds **1**-**3**, 2-methyl-3-oxobutanoyl-*S*-NAC (**4**), and 3-oxohexanoyl-*S*-NAC (**6**) were prepared according to reported protocols[16], as was 2-methyl-3-oxopentanoyl-*S*-NAC (**5**).[17]

To determine MT activity reactions with substrates **1**-**3** (10 mM) contained 150 mM Tris-HCl, 100 mM NaCl, 20 mM SAM, 10% (v/v) glycerol, 20 μM Pfs, and 10 μM MT in a total volume of 200 μL. Reactions were run in parallel at 25 °C for ~16 h. Standards of **4, 5,** and **6** at concentrations from 250 μM to 50 mM were added directly to injection solvent and HPLC peak areas were collected to provide standard curves for observable product formation.

To determine the linear region of MT kinetic data, reactions with substrates **1**-**3** (10 mM) contained 150 mM Tris-HCl, 100 mM NaCl, 20 mM SAM, 10% (v/v) glycerol, 20 μM Pfs, and 10 μM MT in a total volume of 200 μL and were run in parallel at 25 °C and quenched at 0 h, 1 h, 2 h, 3 h, 4 h, and 5 h.

Reactions with substrates **1**-**3** (100 μM, 500 μM, 1 μM, 2.5 mM, 5 mM, 10 mM, or 50 mM) contained 150 mM Tris-HCl, 100 mM NaCl, 20 mM SAM, 10% (v/v) glycerol, 20 μM Pfs, and 10 μM MT in a total volume of 200 μL. Reactions were run in parallel at 25 °C over a period of 1-3 h (MupMT1+**1**, 1 h; MupMT1+**2**, 2 h; MupMT1+**3**, 3 h; BaeMT9+**3**, 2 h; DifMT1+**2**, 2 h; DifMT1+**3**, 2 h) (Figure 2b-g). After completion, reactions were extracted with 1 mL of ethyl acetate. The organic layer was dried *in vacuo* and resuspended in methanol for HPLC analysis. Standard curves were generated by HPLC analysis of 60 μM, 300 μM, 600 μM, 1 μM, 3 mM, and 6 mM injections of **4** and 200 μM, 1 μM, 2 mM, 5 mM, 10 mM, and 20 mM injections of **5** and **6.** Reactions for each set of substrate concentrations were performed in triplicate.

Product formation was quantified by absorbance with reverse phase HPLC resolution of reaction mixtures stopped at a fixed time-point with 0.1 – 50 mM substrate as well as full progress curves at 10 mM substrate (Figure S10). Global fitting of both data sets to a reaction model using Kintek Explorer allowed determination of k_{cat}/K_M values for each enzyme/substrate pair (Table 1 and Figure S1)[18-20].

HPLC analysis was performed with a tandem Waters 2707 autosampler and Waters 1525 binary HPLC pump connected to a Waters 2998 photodiode array detector using a Varian Microsorb-MV C_{18} column (250 × 4.6 mm, 5 μm particle size, 100 Å pore size) and mobile phases consisting of water with 0.1% TFA (solvent A) and acetonitrile with 0.1% TFA (solvent B) with a solvent gradient of 5%-100% B over 30 min at a flow rate of 1 mL/min. High-resolution mass spectrometry measurements of methylated products were obtained by chemical ionization (ESI) with a VG analytical ZAB2-E instrument. Peak integrations were automated with a signal-to-noise cutoff of 5% peak area.

RESULTS AND DISCUSSION

Of the 7 domains cloned, all produced soluble protein with the exception of MupMT3. In addition to several previously identified sequence motifs that distinguish between *cis*- and *trans*-AT MT domains, a *trans*-AT MT sequence alignment revealed an additional notable difference between these two classes of MT domain regarding their position of within the module.[21] In contrast to their *cis*-AT counterparts, *trans*-AT MTs are not embedded within the KR structural subdomain but are instead usually situated immediately after the KR domain and immediately before the ACP domain.[22]

In vitro assays of the excised MTs BaeMT9, DifMT1, and MupMT1 showed each to be capable of catalyzing the methylation of substrates **1, 2,** and **3** to afford **4, 5,** and **6** (Figures 2 and S2-11, Table 1). These results show that, at least when separated from their assembly lines, MTs are not highly substrate-specific. Other excised PKS enzymes [KRs, DHs, ERs and thioesterases (TEs)] also demonstrate broad substrate specificities.[20-25] The low reaction rates of BaeMT9, DifMT1, and MupMT1 are suggestive that local substrate concentrations within the intact assembly line are required for optimal catalytic rates. While the conversions of **1** to **4** catalyzed by BaeMT8 and DifMT1 as well as **2** to **5** catalyzed by BaeMT9 were observed overnight, the percent conversions within the linear region (1-3 h) were too low to accurately report kinetic parameters using HPLC analysis (Figures S5-7). The observed

reaction rates for MTs are lower than those of other excised processing domains (e.g., KRs, DHs, or TEs) towards NAC-linked substrates.[23-28] Although DifMT1 and BaeMT9 demonstrated substrate affinities for **2** and **3** respectively (Table 1), a significant kinetic preference for a specific substrate was not observed from any of the investigated MTs.

The N-terminal MTs DifMT6, DifMT13, and BaeMT14 did not catalyze a detectable amount of methylation of **1**, **2**, or **3**. Unlike the completely embedded MTs, N-terminal MTs may require additional components for activity, such as inclusion in their native polypeptide or interaction with the upstream PKS polypeptide.

The presented work demonstrates that, similar to the other processing domains excised from PKSs, excised *trans*-AT PKS MTs are capable of operating on thioester-bound polyketide substrates *in vitro*. These data disclose the initial investigation of the heretofore unexplored MTs found throughout the *trans*-AT PKS landscape and provide insight into the catalytic activity of the enzyme when removed from its native module. The ability of these MTs to install methyl branches on the carbon chains of small molecule substrates makes them particularly attractive as biocatalysts.

Supplementary Material

Refer to Web version on PubMed Central for supplementary material.

ACKNOWLEDGMENTS

We would like to thank Dr. Kenneth Johnson for helpful discussion pertaining to the fitting of kinetic data. We would also like to thank the University of Texas at Austin mass spectrometry facility for their help in obtaining high-resolution masses for **1**, **2**, **3**, **4**, **5**, **6**. We thank the National Institutes of Health, National Institute of General Medical Sciences (GM106112) and the Welch Foundation (F-1712) for funding.

REFERENCES

1. Piel J. Biosynthesis of polyketides by trans-AT polyketide synthases. Nat. Prod. Rep. 2010; 27:996–1047. [PubMed: 20464003]
2. Helfrich EJ, Piel J. Biosynthesis of polyketides by trans-AT polyketide synthases. Nat. Prod. Rep. 2016; 33:231–316. [PubMed: 26689670]
3. Keatinge-Clay AT. The structures of type I polyketide synthases. Nat. Prod. Rep. 2012; 29:1050–1073. [PubMed: 22858605]
4. Ansari MZ, Sharma J, Gokhale S, Mohanty D. In silico analysis of methyltransferase domains involved in biosynthesis of secondary metabolites. BMC Bioinf. 2008; 9454
5. Liscombe DK, Louie GV, Noel JP. Architectures, mechanisms and molecular evolution of natural product methyltransferases. Nat. Prod. Rep. 2012; 29:1238–1250. [PubMed: 22850796]
6. Miller DA, Luo L, Hillson N, Keating TA, Walsh CT. Yersiniabactin synthetase: a four-protein assembly line producing the nonribosomal peptide/polyketide hybrid siderophore of Yersinia pestis. Chem. Biol. 2002; 9:333–344. [PubMed: 11927258]
7. Poust S, Phelan RM, Deng K, Katz L, Petzold CJ, Keasling JD. Angew. Chem. Int. Ed. 2015; 54:2370.
8. Winter JM, et al. Expanding the structural diversity of polyketides by exploring the cofactor tolerance of an inline methyltransferase domain. Org. Lett. 2013; 15:3775–3777.
9. Cacho RA, et al. Understanding Programming of Fungal Iterative Polyketide Synthases: The Biochemical Basis for Regioselectivity by the Methyltransferase Domain in the Lovastatin Megasynthase. J. Am. Chem. Soc. 2015; 137:15688–15691. [PubMed: 26630357]

10. Jenner M, et al. Substrate specificity in ketosynthase domains from trans-AT polyketide synthases. Angew. Chem. Int. Ed. 2013; 52:1143–1147.
11. Jenner M, et al. Acyl-chain elongation drives ketosynthase substrate selectivity in trans-acyltransferase polyketide synthases. Angew. Chem. Int. Ed. 2015; 54:1817–1821.
12. Moldenhauer J, et al. The final steps of bacillaene biosynthesis in Bacillus amyloliquefaciens FZB42: direct evidence for beta,gamma dehydration by a trans-acyltransferase polyketide synthase. Angew. Chem. Int. Ed. 2010; 49:1465–1467.
13. Chen XH, et al. Structural and functional characterization of three polyketide synthase gene clusters in Bacillus amyloliquefaciens FZB 42. J. Bacteriol. 2006; 188:4024–4036. [PubMed: 16707694]
14. Gurney R, Thomas CM. Mupirocin: biosynthesis, special features and applications of an antibiotic from a gram-negative bacterium. Appl. Microbiol. Biotechnol. 2011; 90:11–21. [PubMed: 21336932]
15. Gay G, Wagner DT, Keatinge-Clay AT, Gay DC. Rapid modification of the pET-28 expression vector for ligation independent cloning using homologous recombination in Saccharomyces cerevisiae. Plasmid. 2014; 7:66–71. [PubMed: 25304917]
16. Piasecki SK, et al. Employing modular polyketide synthase ketoreductases as biocatalysts in the preparative chemoenzymatic syntheses of diketide chiral building blocks. Chem. Biol. 2011; 18:1331–1340. [PubMed: 22035802]
17. Bailey CB, Pasman ME, Keatinge-Clay AT. Substrate structure-activity relationships guide rational engineering of modular polyketide synthase ketoreductases. Chem. Commun. (Camb). 2015; 52:792–795. [PubMed: 26568113]
18. Johnson KA, Simpson ZB, Blom T. Global Kinetic Explorer: A new computer program for dynamic simulation and fitting of kinetic data. Analytical Biochemistry. 2009; 387:20–29. [PubMed: 19154726]
19. Johnson KA, Simpson ZB, Blom T. FitSpace Explorer: An algorithm to evaluate multi-dimensional parameter space in fitting kinetic data. Analytical Biochemistry. 2009; 387:30–41. [PubMed: 19168024]
20. Johnson KA. Fitting enzyme kinetic data with KinTek global kinetic explorer. Computer Methods in Enzymology. 2009; 467:601–626. [PubMed: 19897109]
21. Young J, et al. Elucidation of gephyronic acid biosynthetic pathway revealed unexpected SAM-dependent methylations. J. Nat. Prod. 2013; 76:2269–2276. [PubMed: 24298873]
22. Nguyen T, et al. Exploiting the mosaic structure of trans-acyltransferase polyketide synthases for natural product discovery and pathway dissection. Nat. Biotechnol. 2008; 26:225–233. [PubMed: 18223641]
23. Siskos AP, et al. Molecular basis of Celmer's rules: stereochemistry of catalysis by isolated ketoreductase domains from modular polyketide synthases. Chem. Biol. 2005; 12:1145–1153. [PubMed: 16242657]
24. Li Y, et al. Polyketide intermediate mimics as probes for revealing cryptic stereochemistry of ketoreductase domains. ACS Chem. Biol. 2014; 9:2914–22. [PubMed: 25299319]
25. Wang M, Boddy CN. Examining the role of hydrogen bonding interactions in the substrate specificity for the loading step of polyketide synthase thioesterase domains. Biochemistry. 2008; 47:11793–11803. [PubMed: 18850723]
26. Horsman ME, Hari TP, Boddy CN. Polyketide synthase and non-ribosomal peptide synthetase thioesterase selectivity: logic gate or a victim of fate? Nat. Prod. Rep. 2016; 33:183–202. [PubMed: 25642666]
27. Li Y, et al. Functional Characterization of a Dehydratase Domain from the Pikromycin Polyketide Synthase. J. Am. Chem. Soc. 2015; 137:7003–7006. [PubMed: 26027428]
28. Zheng J, Gay DC, Demeler B, White MA, Keatinge-Clay AT. Divergence of multimodular polyketide synthases revealed by a didomain structure. Nat. Chem. Biol. 2012; 8:615–621. [PubMed: 22634636]

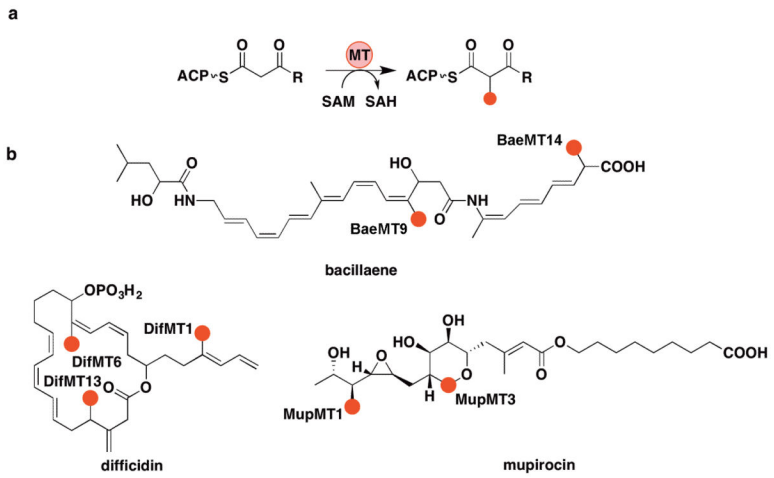

Figure 1.

a) Canonical α-methylation catalyzed by *trans*-AT PKS MTs. b) α-branches and cognate MT domains of bacillaene, difficidin, and mupirocin.

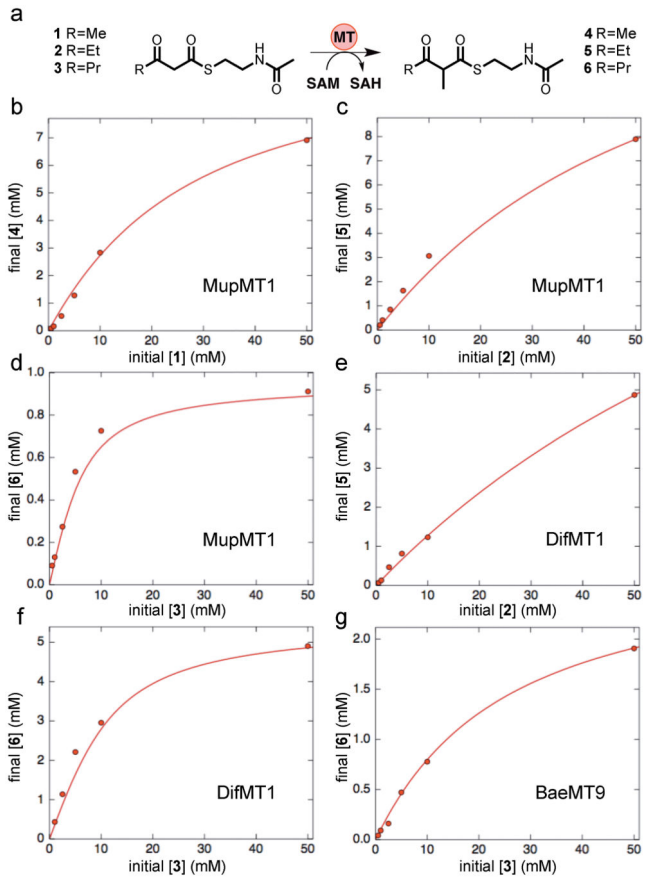

Figure 2.

Saturation curves for a) MupMT1 and **1** after 1 h, b) MupMT1 and **2** after 2 h, c) MupMT1 and **3** after 3 h, d) BaeMT9 and **3** after 2 h, e) DifMT1 and **2** after 2 h, f) DifMT1 and **3** after 2 h. Experimental data from saturation curves was globally fit to a fixed concentration time-course for enzyme-substrate pairs (Figure S1).

Table 1

Kinetic analysis of DifMT1, MupMT1, and BaeMT9 towards N-12 acetylcysteamine substrates.

MT	substrate	k_{cat} (min^{-1})	K_M (mM)	k_{cat}/K_M (mM^{-1} min^{-1})
MupMT1	**1**	26 ± 3.7	22 ± 7	1.2 ± 0.3
MupMT1	**2**	47 ± 14	48 ± 24	1.0 ± 0.4
MupMT1	**3**	4.6 ± 1.6	3.2 ± 3.2	1.5 ± 1.3
DifMT1	**2**	13 ± 5.4	110 ± 83	0.12 ± 0.08
DifMT1	**3**	12 ± 1.9	5.4 ± 3.0	2.2 ± 1.1
BaeMT9	**3**	5.6 ± 2.8	22 ± 19	0.25 ± 0.17